ROBUST STABLE NONLINEAR CONTROL AND DESIGN OF A CSTR IN A LARGE OPERATING RANGE

Johannes Gerhard, Martin Mönnigmann, Wolfgang Marquardt

Lehrstuhl für Prozesstechnik, RWTH Aachen
Turmstr. 46, D-52064 Aachen, Germany

Abstract: In this work an approach based on nonlinear dynamics is used for the integrated design and controller tuning of a CSTR. The approach enables integrated design optimization and robust tuning of a linearizing feedback controller. The controller setting found by the approach guarantees robust stability of the process over a large range of set point variations even in the presence of parameter uncertainty. The method enforces robust stability by introducing lower bounds on the parametric distance of the operating point to critical boundaries in the space of process and controller parameters. For stabilization of a large range of operations, a lower bound on the distance to a nontransversal Hopf bifurcation has to be considered in this particular case.

1. INTRODUCTION

Chemical processes generally exhibit nonlinear behavior. In process and control design it is of particular importance to guarantee stable behavior of the closed-loop process. Ideally, the operating point should be robust against uncertainties in the underlying process model. For nonlinear chemical processes with a frequently changing set point it is furthermore desirable to guarantee robust stability over a wide range of operating conditions.

In this paper the issue of robust stability over a wide range of operating conditions is discussed for a temperature controlled CSTR (continuously stirred tank reactor). Control is realized by linearizing feedback control. A bifurcation analysis of the CSTR performed by Hahn *et al.* (2003) shows that model uncertainties may lead to unstable operating points for a particular range of set points. The analysis also reveals that a lower bound of the control parameter exists above which the unstable region vanishes completely. This behavior can be attributed to a so-called nontransversal Hopf bifurcation.

In this work a novel design method based on nonlinear dynamics and bifurcation theory is adopted and used for an integrated process design and controller tuning of a CSTR. The method has been reported recently by Mönnigmann and Marquardt (2002a, 2003). It enables the optimization of process systems with respect to some profit function guaranteeing robust stability in the presence of parametric uncertainty. The method is applicable to both open and closed-loop systems. In case of the CSTR considered, stability is ensured by maintaining a specified lower bound on the distance between the operating point and the critical boundary formed by the set of all nontransversal Hopf points. Results of the approach are presented for two illustrating design scenarios.

2. PROCESS MODEL AND LINEARIZING FEEDBACK CONTROLLER

We consider a cooled CSTR with an exothermic first order reaction $A \rightarrow B$. Assuming perfect level control, the CSTR model consists of the material and energy balances. It reads

$$\begin{aligned}\dot{c_A} &= \frac{q}{V}(c_{Af} - c_A) - \Delta k_0 \exp\left(-\frac{E}{RT}\right) c_A\,,\\ \dot{T} &= \frac{q}{V}(T_f - T) - \frac{\Delta H k_0}{\rho C_p} \exp\left(-\frac{E}{RT}\right) c_A \\ &\quad + \frac{UA}{V\rho C_p}(T_c - T)\,.\end{aligned} \tag{1}$$

The temperature of the cooling fluid T_c is the manipulated variable and the reactor temperature T is the measured and controlled variable (Uppal *et al.*, 1974).

Control is realized by means of linearizing feedback including integral action. The control law reads as (Hahn *et al.*, 2003)

$$\begin{aligned}u = &\frac{-\frac{q}{V}(T_f - T) + \frac{\Delta H}{\rho C_p} k_0 \exp(-\frac{E}{RT}) c_A + \frac{UA}{V\rho C_p} T}{\frac{UA}{V\rho C_p}} \\ &+ \frac{\frac{2}{\epsilon}(T_{sp} - T) + \frac{1}{\epsilon^2}\int_0^t (T_{sp} - T) d\tau}{\frac{UA}{V\rho C_p}}\,.\end{aligned} \tag{2}$$

The tuning parameter ϵ corresponds to the time constant of the closed loop dynamics, i. e. the smaller ϵ the faster is the dynamics of the closed loop. The integral action $1/\epsilon^2 \int_0^t (T_{sp} - T) d\tau$ is included to compensate for potential set point offsets.

3. BIFURCATION ANALYSIS

In a previous article (Hahn *et al.*, 2003) the closed loop process model (1), (2) has been analyzed by parameter continuation and bifurcation theory in the presence of unmodeled dynamics and parametric uncertainties. Unmodeled dynamics have been introduced into the model by an overdamped second order process between the controller output u and the manipulated variable T_c according to

$$\begin{aligned}\epsilon_v \dot{z} &= -u + z\\ \epsilon_v \dot{T_c} &= -T_c + z\,,\end{aligned} \tag{3}$$

where ϵ_v represents the unknown time constant of the unmodeled dynamics. The controller (2) remains unchanged. The assumed value of ϵ_v and the other process parameters are summarized in Table 1.

Table 1. Parameters used for analysis

Parameter	Value	Parameter	Value
ΔH	$-5 \cdot 10^4\ \frac{\mathrm{J}}{\mathrm{mol}}$	$\frac{E}{R}$	8750 K
c_{Af}	$1\ \frac{\mathrm{mol}}{\mathrm{l}}$	k_0	$7.2 \cdot 10^{10}\ \frac{1}{\mathrm{min}}$
T_f	350 K	UA	$833.3\ \frac{\mathrm{W}}{\mathrm{K}}$
V	100 L	C_p	$0.239\ \frac{\mathrm{J}}{\mathrm{gK}}$
ρ	$1000\ \frac{\mathrm{g}}{\mathrm{l}}$	q	$100\ \frac{\mathrm{mol}}{\mathrm{min}}$
ϵ_v	0.05 min		

The results of the analysis are briefly summarized here in order to assert the existence of a particular critical point, a so-called nontransversal Hopf (NTH) bifurcation, which fully controls the stability loss in this case. Thus the design approach presented in Section 4 can solely be based on this NTH bifurcation.

Continuation of the equilibria from a stable operating point with varying set point temperature T_{sp} yields two Hopf bifurcations. The Hopf

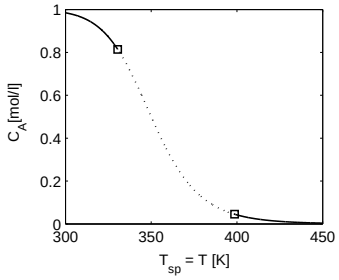

Fig. 1. Curve of steady states for variations in T_{sp}. Two Hopf bifurcations (□) divide the curve into stable states (solid line) and unstable states (dotted line).

points separate the curve of steady states shown in Fig. 1 into two stable parts, and an unstable part between the two stable parts. Introducing the control parameter ϵ as a second free parameter, a curve of Hopf points can be evaluated. This

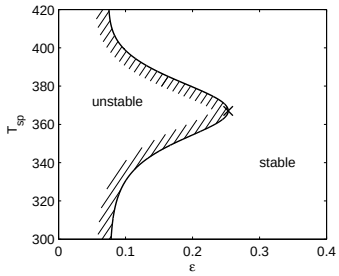

Fig. 2. Curve of Hopf points and nontransversal Hopf point (×) at $\epsilon = 0.25$ min.

curve of Hopf points shown in Fig. 2 separates the parameter space (ϵ, T_{sp}) into a stable and an unstable region. The distance between the two Hopf points diminishes with increasing values of ϵ. At $\epsilon = 0.25$min, $T_{sp} = 367$K, they merge and form an extremum with respect to the control parameter ϵ.

The bifurcation at the extremum of the Hopf curve is the already mentioned NTH bifurcation. The NTH point represents a lower boundary for the robust tuning of the controller. For values of ϵ larger than the extremal value, stability can be guaranteed for *all* values of T_{sp}. Hence the process is stable over the entire range of operating conditions of interest.

4. CONTROL SYNTHESIS FOR STABILITY

This section gives a short introduction into the basic idea of the design method. For a rigorous

derivation of the method the reader is referred to Mönnigmann and Marquardt (2002a). The method is applied to the NTH bifurcation which was found by means of continuation analysis of the process. The dynamic equations of the process model (1), the controller (2) and the unmodeled dynamics (3) are denoted by

$$\dot{x} = f(x, \alpha, p)\,, \quad x(t_0) = x_0\,. \tag{4}$$

In this notation, $x \in \mathbb{R}^{n_x}$ are the state variables, $\alpha \in \mathbb{R}^{n_\alpha}$ the uncertain process and controller parameters and $p \in \mathbb{R}^{n_p}$ the known parameters.

The robustness of the operating point has to be guaranteed only for the uncertain parameters of the process model. It is assumed that there are known upper and lower uncertainty boundaries $\pm\Delta\alpha$ for all α, i. e.

$$\alpha_i \in \left[\alpha_i^{(0)} - \Delta\alpha_i,\, \alpha_i^{(0)} + \Delta\alpha_i\right]\,,\; i = 1, \ldots, n_\alpha\,.$$

These boundaries are defined e. g. by the accuracy of measurements. The scaling of the parameters

$$\alpha_i \to \frac{\alpha_i}{\Delta\alpha_i},\; \alpha_i^{(0)} \to \frac{\alpha_i^{(0)}}{\Delta\alpha_i}$$

gives the dimensionless parameters

$$\alpha_i \in \left[\alpha_i^{(0)} - 1, \alpha_i^{(0)} + 1\right]\,. \tag{5}$$

Robustness against the uncertainties is achieved by enforcing a minimal distance between the critical manifold and the operating point in the space of uncertain parameters. The minimal distance is equal to the radius $\sqrt{n_\alpha}$ of the n_α-dimensional ball enclosing the n_α-dimensional cube of sidelength 2 defined by eq. (5). In Fig. 3, a robust operating point is shown for $n_\alpha = 2$. The ball with a radius

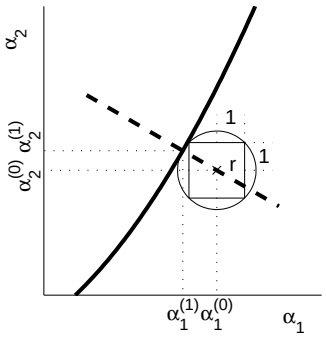

Fig. 3. Robust operating point $\alpha^{(0)}$ with stability boundary (thick line). The critical point $\alpha^{(1)}$ nearest to the operating point is in the direction of the normal vector r (dashed thick line) at a distance of $\sqrt{2}$ from $\alpha^{(0)}$.

of $\sqrt{2}$ touches the critical boundary tangentially guaranteeing stability for the nominal operating point $\alpha_i^{(0)}$ and for all variations of the parameters within their range of uncertainty. The minimal distance $l = \sqrt{n_\alpha}$ between the critical manifold and the operating point occurs along the direction of the normal vector r to the critical manifold. Thus the constraints for the robustness are given by

$$\alpha^{(0)} = \alpha^{(1)} + l\frac{r}{\|r\|} \tag{6}$$

$$l \geq \sqrt{n_\alpha}\,. \tag{7}$$

A scheme for the derivation of the system of equations defining r for a generalized critical point has been derived by Mönnigmann and Marquardt (2002a). The NTH point that is found in the bifurcation analysis of the reactor model is a degenerated Hopf point. Thus the normal vector system of the NTH point can be derived from the normal vector system of a regular Hopf point. According to Mönnigmann and Marquardt (2002a) the augmented system for the normal vector r on a Hopf point is given by

$$0 = f(x, p, \alpha) \tag{8a}$$

$$\begin{aligned} 0 &= f_x w^{(1)} + \omega w^{(2)} \\ 0 &= f_x w^{(2)} - \omega w^{(1)} \\ 0 &= w^{(1)T} w^{(1)} + w^{(2)T} w^{(2)} - 1 \\ 0 &= w^{(1)T} w^{(2)} \end{aligned} \tag{8b}$$

$$\begin{aligned} 0 &= f_x^T v^{(1)} - \omega v^{(2)} + \gamma_1 w^{(1)} - \gamma_2 w^{(2)} \\ 0 &= f_x^T v^{(2)} + \omega v^{(1)} + \gamma_1 w^{(2)} + \gamma_2 w^{(1)} \\ 0 &= v^{(1)T} w^{(1)} + v^{(2)T} w^{(2)} - 1 \\ 0 &= v^{(1)T} w^{(2)} - v^{(2)T} w^{(1)} \\ 0 &= f_x^T u + v^{(1)T} f_{xx} w^{(1)} + v^{(2)T} f_{xx} w^{(2)} \end{aligned} \tag{8c}$$

$$\begin{aligned} 0 = r &- f_\alpha^T u - v^{(1)T} f_{x\alpha} w^{(1)} \\ &- v^{(2)T} f_{x\alpha} w^{(2)}\,. \end{aligned} \tag{8d}$$

The system of equations (8) is divided into four parts. Eqns. (8a) define the steady state of the process. Eqns. (8b) denote the augmented system for Hopf bifurcations, with f_x being the Jacobian of the model equations, $i\omega$ the eigenvalue of the Jacobian with vanishing real part and $w^{(1)} + iw^{(2)}$ the corresponding complex eigenvector. Eqns. (8c) introduce the complex eigenvector $v^{(1)} + iv^{(2)}$ corresponding to f_x^T and the eigenvalue $-i\omega$, and the auxiliary variables u, γ_1 and γ_2 for the calculation of the normal vector r given by eqns. (8d).

It is easy to derive the normal vector system for the NTH point by means of a geometric argument. From the curve of Hopf points in Fig. 2 it is obvious that the component of the normal vector in direction of T_{sp}, $r_{T_{sp}}$, is equal to zero at the extremum of the curve. The system that defines the normal vector of the NTH point is therefore identical to the set of equations (8) except for the subsystem (8d) that contains $r_{T_{sp}}$. Without restrictions it is assumed that $T_{sp} = \alpha_1$. Then the eqns. (8d) have to be replaced by

$$
\begin{aligned}
0 &= f_{\alpha_1}^T u + v^{(1)T} f_{x\alpha_1} w^{(1)} + v^{(2)T} f_{x\alpha_1} w^{(2)} \\
0 &= r - f_{\alpha_i}^T u - v^{(1)T} f_{x\alpha_i} w^{(1)} \\
&\quad - v^{(2)T} f_{x\alpha_i} w^{(2)}\,, \qquad i = 2, \ldots, n_\alpha\,.
\end{aligned} \tag{9}
$$

The equations defining the normal vector on the NTH bifurcation (8a)–(8c), (9) are summarized by

$$
G(x, \tilde{x}, p, \alpha, r) = 0, \tag{10}
$$

where $\tilde{x}$ denotes the auxiliary variables (e. g. w, v, u). Together with the eqns. (6) and (7) that define the minimal distance between an operating point $(x^{(0)}, \alpha^{(0)}, p^{(0)})$ and a critical point $(x^{(1)}, \alpha^{(1)}, p^{(1)})$, eqns. (10) represent the necessary constraints that must hold in order to guarantee robust stability for a large range of operating conditions. Thus the robust optimum of the process model (4) with respect to a cost function ϕ can be found by solving the following constrained nonlinear programm

$$
\min_{x^{(0)}, \alpha^{(0)}, p^{(0)}} \phi(x^{(0)}, \alpha^{(0)}, p^{(0)}) \tag{11a}
$$

$$
\text{s. t.} \qquad 0 = f(x^{(0)}, \alpha^{(0)}, p^{(0)})\,, \tag{11b}
$$

$$
\begin{aligned}
0 &= G(x^{(1)}, \tilde{x}^{(1)}, \alpha^{(1)}, p^{(1)}, r)\,, \\
0 &= \alpha^{(1)} - \alpha^{(0)} + l \frac{r}{\|r\|}\,, \\
0 &\leq l - \sqrt{n_\alpha}\,.
\end{aligned} \tag{11c}
$$

Eqns. (11b) ensure that the optimal operating point is a steady state of the process model. The constraints (11c) enforce the minimal distance of the optimum to the critical points. It is important to note that certain restrictions (Mönnigmann and Marquardt, 2003) must hold for the system (4) in order to apply the normal vector approach. In particular it has to be assumed that variations of the uncertain parameters are slow compared to the time scales of the process, i. e. all α may only vary quasistatically with respect to the system dynamics.

5. ILLUSTRATIVE EXAMPLES

In this section the theory described above will be illustrated by two exemplary integrated design and control problems associated with the CSTR. In the first example, the design problem is the maximization of the reactor yield. The control problem consists of finding a robust controller setting that not only stabilizes the optimal operating point but furthermore allows set point variations without loss of stability. The robustness against set point variations is crucial for a reactor with frequently varying demands on the product quality. The design problem in the second example addresses the minimization of the investment costs attributed to the heat transfer area for a fixed rate of production. The control design problem is again to find a robust controller setting for the optimal reactor design that allows for setpoint variations without loss of stability. The constrained optimization problem (11) is used for the solution of both integrated problems. From a technical point of view, (11) guarantees the robust stability for all values of the parameter T_{sp} by ensuring a specified distance to the manifold of NTH bifurcations. For both examples, results of the optimization without the robustness constraints (11c) are included for reference.

5.1 Optimization of the reactor yield

Here the CSTR is optimized with respect to the amount of B produced per unit time. The production of B is equivalent to the amount of converted A. The function to be maximized is therefore chosen to be

$$
\phi = q\,(c_{Af} - c_A) \tag{12}
$$

with a constant concentration $c_{Af} = 1.0\,\mathrm{mol/l}$ of the feed. The objective function may be increased by increasing the feed rate q or decreasing c_A. A decrease of c_A can be achieved by setting the reactor temperature $T = T_{sp}$ to higher values. To ensure the thermal stability of the product it is therefore necessary to impose an upper bound on T_{sp}. Assuming that water is used as the cooling medium a lower bound has to be set on T_c. For the optimization problem these bounds represent additional constraints, e. g.

$$
\begin{aligned}
T_{\max} &\leq 400\mathrm{K}\,, \\
T_{c,\min} &\geq 300\mathrm{K}\,.
\end{aligned} \tag{13}
$$

The time constant ϵ_v of the unmodeled dynamics and the feed rate q are assumed to be the uncertain parameters ($n_\alpha = 2$). The uncertainties are set to

$$
\begin{aligned}
\Delta q &= 10\,\mathrm{mol/min}\,, \\
\Delta \epsilon_v &= 0.01\mathrm{min}\,,
\end{aligned} \tag{14}
$$

which correspond to 10% and 20% of the nominal values given in Table 1, respectively. While the nominal value of q may vary, the estimated nominal value of $\epsilon_v = 0.05\,\mathrm{min}$ is assumed to be constant. T_{sp} and the controller parameter ϵ are known parameters ($n_p = 2$) of the optimization problem (11).

For reference, the results for the optimization without any normal vector constraints are shown in Fig. 4. For this optimization run the control parameter ϵ is fixed at the value $\epsilon = 0.25\,\mathrm{min}$ corresponding to the NTH bifurcation found in the analysis given in Section 3. The figure shows that the operating point is on the wrong side of the robustness boundary. The optimal operating point itself is stable, but continuation analysis reveals that variations of T_{sp} result in unstable operating points between $352.0\,\mathrm{K} < T_{sp} < 388.3\,\mathrm{K}$.

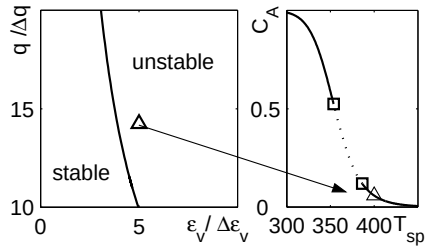

Fig. 4. Left: Nonrobust optimum (△) at maximum yield. Right: Continuation analysis reveals two Hopf bifurcations (□) and an unstable region (dotted).

To achieve the required stability over the entire range of T_{sp} an optimization including the normal vector constraints (11c) has to be carried out. Fig. 5 illustrates the obtained result. The robustness circle with the radius $r = \sqrt{n_\alpha} = \sqrt{2}$ around the optimal operating point touches the critical boundary. Variations of T_{sp} confirm that the setting of the control parameter found, $\epsilon = 2.28\,\mathrm{min}$, guarantees stability for the entire region of operating conditions.

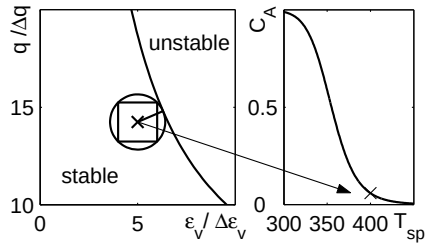

Fig. 5. Left: Robust optimum (×) at maximum reactor yield. Right: Continuation analysis shows stability for all T_{sp}.

The values of the objective function are the same for both optimizations. The two operating points only differ in the value of the controller parameter ϵ. The cost function (12) obviously defines the reactor parameters and the normal vector constraints (11c) define the controller parameter in the optimization problem. Comparing both stability boundaries it becomes obvious that the higher value of ϵ enlarges the region of stable parameter settings. Loosely speaking the normal vector constraints shift the critical boundary by increasing ϵ until the optimal operating point is found on the robust side of the boundary. The constraints guarantee that no NTH bifurcation occurs for any variations of the uncertain parameters within their specified uncertainties. The drawback for the stabilization of the entire range of operating points is the conservative setting of ϵ. If only robust stabilization of the optimal set point is required much tighter control becomes feasible.

The optimal robust parameter settings are summarized in Table 2. The temperature constraints (13) are both active at the optimum.

Table 2. Robust optimal operating point

Parameter	Value	Parameter	Value
q	$142.4\,\frac{\mathrm{l}}{\mathrm{min}}$	ϵ	$2.28\,\mathrm{min}$
T_c	$300.0\,\mathrm{K}$	$T_{sp} = T$	$400.0\,\mathrm{K}$
c_A	$0.06\,\frac{\mathrm{mol}}{\mathrm{l}}$	ϕ	$134.0\,\frac{\mathrm{mol}}{\mathrm{min}}$

5.2 Minimization of the heat transfer area

The aim of the optimization is to find an optimal reactor design that produces a specified amount of B with minimized investment cost and a controller setting that allows for variations of the set point temperature without loss of stability. The objective function is given by the investment cost attributed to the heat transfer area. According to Douglas (1990) they can be estimated to be

$$\phi = 2285 A^{0.65} [\$]\,, \tag{15}$$

with A in m^2. Here a constant heat transfer coefficient $U = 100\,\mathrm{W/m^2K}$ is assumed. The value of (15) is only influenced by UA which becomes an additional parameter for the optimization problem in this example. However, it is not possible to set UA to arbitrary small values since the constraints on the reactor temperature and cooling water temperature (13) apply to this optimization problem as well. The desired production rate of B is arbitrarily set to be

$$q(c_{Af} - c_A) = 85\,\mathrm{mol/min}\,. \tag{16}$$

UA is assumed to be uncertain. The uncertainty is set to

$$\Delta UA = 83.3\,\mathrm{W/K}\,, \tag{17}$$

which corresponds to 10% of the nominal value given in Table 1. Together with the uncertainties Δq and $\Delta\epsilon_v$ specified in eq. (14), there are three uncertain parameters ($n_\alpha = 3$) and two known parameters (ϵ and T_{sp}, $n_p = 2$) in this optimization problem. The desired production rate (16) constitutes an additional equality constraint.

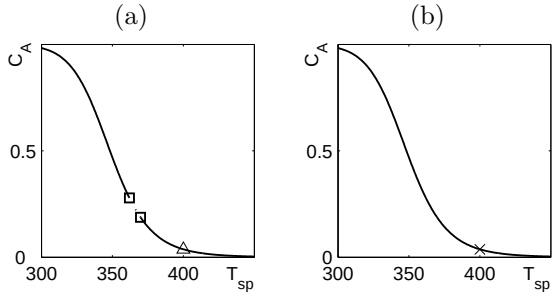

Fig. 6. (a) Continuation of the non robust optimum (△) with two Hopf bifurcations (□) and an unstable region (dotted). (b) Continuation of the robust optimum (×) yields set of stable operating points.

For reference, results without normal vector constraints are shown in Fig. 6a. The controller parameter is set to $\epsilon = 0.25\,\mathrm{min}$. As in the previous

example this optimization results in a stable operating point. Variations of T_{sp}, however, again give rise to Hopf bifurcations and a region of unstable operating points at $360.5\,\mathrm{K} < T_{sp} < 371.3\,\mathrm{K}$.

The required stability for all values of T_{sp} at the optimal reactor design is obtained by including the normal vector constraints in the optimization problem.

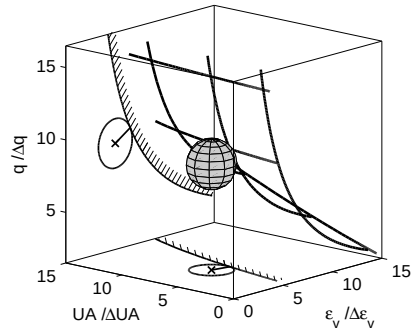

Fig. 7. Robust optimization with cost function (15); the operating point is surrounded by its robustness sphere; the critical manifold is indicated by thick lines; the optimal operation point, the robustness sphere and the critical manifold are projected onto the planes (ϵ_v, q) and (ϵ_v, UA).

Fig. 7 shows the robust operating point with the controller setting of $\epsilon = 0.63\,\mathrm{min}$ in relation to the critical boundary spanned by the uncertain parameters ϵ_v, q and UA. The robustness sphere with the radius $r = \sqrt{3}$ around the operating point touches the critical manifold. Thus it is guaranteed that no NTH bifurcation occurs within the specified range of uncertainties. As in the previous example, the value of the objective function (15) corresponds to the value obtained without the robustness constraints. Robust stability is achieved by increasing ϵ. The continuation analysis in Fig. 6b shows the desired stability over the entire range of T_{sp}. The results of the optimized operating point are summarized in Table 3. The determined reactor design admits a faster control in comparison with the control of the robust maximum of the reactor yield. Relaxing the robustness requirements to solely stabilizing the optimal operating point, however, would admit even tighter control.

Table 3. Robust optimal operating point

Parameter	Value	Parameter	Value
q	$88.3\,\frac{\mathrm{l}}{\mathrm{min}}$	c_A	$0.04\,\frac{\mathrm{mol}}{\mathrm{l}}$
$q(c_{Af} - c_A)$	$85\,\frac{\mathrm{mol}}{\mathrm{min}}$	ϵ	$0.63\,\mathrm{min}$
$T_{sp} = T$	$400.0\,\mathrm{K}$	T_c	$300.0\,\mathrm{K}$
UA	$532.5\,\frac{\mathrm{W}}{\mathrm{K}}$	ϕ	6776 \$

6. CONCLUSIONS

In this paper, an integrated method of robust design optimization and controller tuning for a temperature controlled CSTR is presented. The controller is realized by means of linearizing feedback. The integrated method guarantees stability of the optimal operating point for variations of uncertain parameters within specified bounds and for all variations of the set point. Robust stability is achieved by constraints that ensure a specified distance in the direction of the normal vector from the operating point to a critical boundary of NTH bifurcations. The critical boundary separates the parameter space into one region where set point variations always result in a stable operating point and another region where variations of the set point give rise to instabilities. For an extension of the method to constraints that guarantee not only stability but also a specified performance of the closed loop system the reader is referred to Mönnigmann and Marquardt (2002b). In this work critical manifolds of steady states are considered at which the real part of the leading eigenvalue attains a user specified value $\sigma_0 < 0$.

Clearly the presented integrated design method is neither restricted to the simple examples presented nor to linearizing feedback control. It can be applied to any process that exhibits a NTH bifurcation controlling the stability loss, if stability has to be guaranteed in the presence of uncertainties even in a large region of operating conditions.

REFERENCES

Douglas, J.M. (1988). *Conceptual Design of Chemical Processes*. 1994. 2nd ed.. McGraw-Hill. New York.

Hahn, J. M. Mönnigmann and W. Marquardt (2003). Robust tuning of feedback linearizing controllers via bifurcation analysis. In: *Proceedings of ADCHEM 2003, Hong Kong, China*. pp. 525–530.

Mönnigmann, M. and W. Marquardt (2002*a*). Normal vectors on manifolds of critical points for parametric robustness of equilibrium solutions of ODE systems. *Journal of Nonlinear Science* **12**, 85–112.

Mönnigmann, M. and W. Marquardt (2002*b*). Parametrically robust control-integrated design of nonlinear systems. In: *Proceedings of the American Control Conference 2002 (6), IEEE*. pp. 4321–4326.

Mönnigmann, M. and W. Marquardt (2003). Steady state process optimization with guaranteed robust stability and robust feasibility. *AIChE J.* **49**, 3110–3126.

Uppal, A. W.H. Ray and A.B. Poore (1974). On the dynamic behavior of continuous stirred tank reactors. *Chem. Eng. Sci.* **29**, 967–985.